A Force to Be Reckoned With: A Review of Synthetic Microswimmers Powered by Ultrasound

K. Jagajjanani Rao, Fei Li, Long Meng, Hairong Zheng, Feiyan Cai, and Wei Wang**

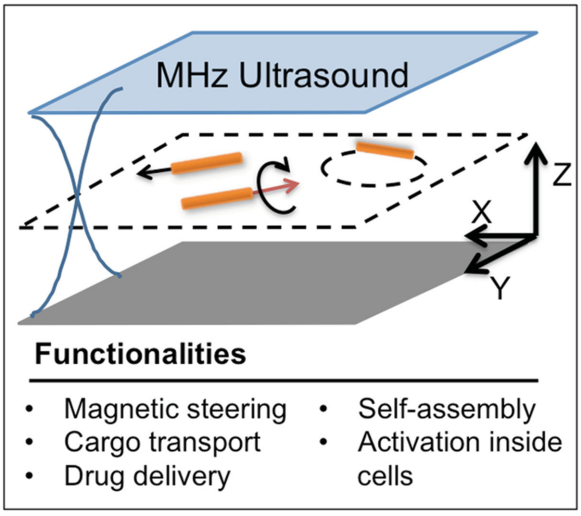

From the Contents

Synthetic microswimmers are a class of artificial nano- or microscale particle capable of converting external energy into motion. They are similar to natural microswimmers such as bacteria in behavior and are, therefore, of great interest to the study of active matter. Additionally, microswimmers show promise in applications ranging from bioanalytics and environmental monitoring to particle separation and drug delivery. However, since their sizes are on the nano-/microscale and their speeds are in the μm s^{-1} range, they fall into a low Reynolds number regime where viscosity dominates. Therefore, new propulsion schemes are needed for these microswimmers to be able to efficiently move. Furthermore, many of the hotly pursued applications call for innovations in the next phase of development of biocompatible microswimmers. In this review, the latest developments of microswimmers powered by ultrasound are presented. Ultrasound, especially at MHz frequencies, does little harm to biological samples and provides an advantageous and well-controlled means to efficiently power microswimmers. By critically reviewing the recent progress in this research field, an introduction of how ultrasound propels colloidal particles into autonomous motion is presented, as well as how this propulsion can be used to achieve preliminary but promising applications.

DOI: 10.1002/smll.201403621

1. Introduction

Autonomous and functional machines operating at the nano- or microscale have long been the dream of human beings.[1,2] Envisioned by Nobel Physics laureate Richard Feynman,[3] and later popularized by the 1966 movie Fantastic Voyage[4] and the more recent concepts of molecular assemblers,[5] these small machines, often referred to (by researchers from different fields of study) as microswimmers, microrobots, colloidal motors, or nanomotors, are expected to serve humanity in a variety of ways including drug delivery, noninvasive surgery, and the assembly of materials at the nanoscale, to name a few.[6–11] Despite the long-standing visions, the successful experimental realization of such small devices has met a number of serious challenges, a major one of which being to achieve autonomous motion at such small length scales.

Similar to their macroscale counterparts, machines at the nano- and microscale need energy to move. Popular mechanisms employed by macroscale machines such as gliding and reciprocal motion are not particularly useful to microswimmers, due to the restraints placed on them by extremely small Reynolds numbers (*Re*), which characterizes the relative magnitude of inertia vs. viscous drag forces ($\approx 10^{-5}$ for a bacteria of 1 μm in size swimming at 10 μm s^{-1} in water). At such small *Re*, the motion of an object stops almost immediately after the pushing force is removed due to strong viscous drags. Since inertia hardly plays a role at low *Re*, reciprocal motion only results in zero net displacement, i.e., the movement due to the forward component of the motion will be cancelled by that from the backward component of the motion.[12] As a result, completely different propulsion mechanisms need to be developed to effectively move the particles. Although external electromagnetic fields have been demonstrated to align and move microparticles,[13–16] the first demonstration of synthetic colloidal particles capable of autonomous motion originated from research teams at Penn State University and the University of Toronto around 2004, who independently discovered that bimetallic microrods autonomously move in hydrogen peroxide solutions.[17,18] This discovery sparked imagination among scientists and engineers, and over the last ten years it has lead to many research accomplishments that attracted intensive interest (the reader may refer to other review articles for further details[8,9,11,19,20]).

Thus far, environmental cues such as chemical gradients and chemical reactions,[19,21–32] magnetic,[33–38] electric,[39–48] light,[49–56] sound,[57,58] and temperature gradients[59–61] have been successfully used to power synthetic nano- and microswimmers. However, very few of them meet the requirements of the ideal energy source for powering nano-/microscale machines, especially for biomedical applications which are most heatedly anticipated for these devices. In **Table 1** we compare the working pinciples, advantages, and limitations of a few common microswimmer systems (please note that only one or two references are given for each microswimmer type as an example; more examples are available in the comprehensive review articles mentioned above). Ideally, a microswimmer needs to be able to swim in a biologically relevant environment (typically of high viscosity and high ionic strength) at high speeds driven by a biocompatible energy source (toxic chemicals are therefore eliminated as fuel candidates).[62–64] Additionally, it is highly preferable that these microswimmers can either be externally steered (often by magnetic fields) or autonomously find their way towards the target. These strict requirements have served as the main motivation to develop better ways to power micromachines.

Among the various ways that have been developed to provide energy to nano- and microdevices, two have emerged as more promising in meeting the above requirements: magnetic fields and ultrasound. Magnetic fields were first exploited to induce motion in a flexible chain of microparticles linked by DNA in 2005,[33] and subsequent research has made much improvement based on similar effects.[35–37] In a typical system of magnetically propelled micromachines, helix-shaped ferromagnetic colloidal particles mimic bacterial flagella by responding to an external and rotating magnetic field. Their body rotation translates into a directional motion, which can reach a peak velocity of roughly 10 body lengths per second at a magnetic field strength of less than 10 mT. The current research effort on a number of variations based on this principle is primarily focused on achieving faster and more efficient propulsion by experimental setups as simply as possible, as well as some preliminary biomedical explorations.[65,66]

Using ultrasound, especially MHz ultrasound, to power nano-/microscale machines is a fairly new idea that was first developed in 2012 by Mallouk, Hoyos, and co-workers. In their experiment, metallic microrods were demonstrated to move autonomously in aqueous solutions in standing ultrasound waves operated at MHz frequencies, at speeds as high as 200 μm s^{-1} (≈70 body lengths per second).[57] Additionally, chaining, spinning, and rotation were observed with these metallic microrods. This interesting phenomenon immediately attracted a significant amount of attention within the scientific community, and have served as the foundation for a series of reports that include preliminary studies of drug delivery with functionalized ultrasound-powered microswimmers,[67] and activation of ultrasound-powered microswimmers inside living cells.[68] Furthermore, different theories regarding how ultrasound induces autonomous motion have

Dr. K. J. Rao, Prof. W. Wang
School of Materials Science and Engineering
Harbin Institute of Technology
Shenzhen Graduate School
Shenzhen 518055, PR China
E-mail: wwang@hitsz.edu.cn

Dr. K. J. Rao
Interfaces and Nanomaterials Laboratory
Department of Chemical Engineering
National Institute of Technology
Rourkela–769 008, Orissa, India

Dr. F. Li, Dr. L. Meng, Prof. H. Zheng, Dr. F. Cai
Paul C. Lauterbur Research Center for Biomedical Imaging
Institute of Biomedical and Health Engineering
Shenzhen Institutes of Advanced Technology
Chinese Academy of Sciences
Shenzhen 518055, P.R. China
E-mail: fy.cai@siat.ac.cn

DOI: 10.1002/smll.201403621

been proposed.[69–71] Although both magnetic and ultrasonic propulsion of microswimmers are biocompatible (at appropriate power levels), powering micromachines with MHz ultrasound has a few unique advantages. In particular, compared to powering magnetic helical particles with rotating magnets, colloidal particles propelled by ultrasound can be made of more shapes (shape asymmetry required) and compositions (not necessarily magnetic), and the experimental setup and the sample fabrication process are both simpler. These advantages greatly expand the usability of this technique.

It is worth noting that there exist different classes of synthetic systems that can move at the nano- and microscale, such as DNA and molecular motors, and nano- (and micro-) electromechanical systems (NEMS and MEMS).[72–74] These systems, with their unique features, capabilities, applications, and challenges, are beyond the scope of this review article as well as the general theme of synthetic microswimmers. The microswimmers of interest in this article are typically larger in size (hundreds of nanometers to tens of micrometers), more powerful, and move faster, with speeds in the range of μm s^{-1} to even mm^{-1}.

In this review article, the authors would like to provide the readers with a quick overview of the young and dynamic research field of ultrasonically propelled microswimmers. We start by introducing some key concepts relating to how ultrasound can manipulate microparticles, which are the essential background knowledge to understand the behavior of microswimmers in an acoustic field. We then critically review the recent progress made in this research field, followed by concluding with a comment on the research challenges. As the first review article that is specifically dedicated to microswimmers powered by ultrasound, in our sincere hope, this article will provide useful information and insights to experienced microswimmer researchers and interested readers alike.

2. Basic Theories of the Ultrasonic Manipulation of Microparticles

A microparticle in a sound field that absorbs, scatters, or reflects sound is subjected to an acoustic radiation force, and thus can be manipulated without contact.[81,82] Since the magnitude of the acoustic radiation force on a microparticle in a standing wave is much larger than that in a travelling wave, research into acoustic propulsion and manipulation are mostly carried out in a standing acoustic field.[83–85] Standing waves are formed following the criteria below,

$$h = \frac{1}{2} n \cdot \lambda = \frac{1}{2} n \cdot \frac{c}{f} \quad n = 1, 2, 3\ldots \tag{1}$$

where h is the height of the acoustic chamber (acoustic path length), λ is the wavelength, f is the frequency, n is an integer, and c is the speed of sound in the medium (c = 1492 m s^{-1} in deionized water).

In standing waves, the acoustic pressure nodes and antinodes are the local potential extrema. The acoustic radiation force on a microparticle located at r can be expressed by[86]

Feiyan Cai received her PhD from the Department of Physics at Wuhan University, China, in 2008. Then she joined the Shenzhen Institutes of Advanced Technology (SIAT), Chinese Academy of Sciences, as an an assistant professor. Currently she is an associate professor at SIAT. Her research interests include acoustic manipulation, acoustofluidics, and phononic crystals.

Wei Wang graduated from the Harbin Institute of Technology in 2008 with a Bachelor Degree in Science. He then went to the Pennsylvania State University (USA) where he pursued a PhD in chemistry under the supervision of Prof. T. E. Mallouk. After receiving his PhD he returned to China in 2013, where he is now an associate professor in the School of Materials Science and Technology in the Harbin Institute of Technology, Shenzhen Graduate School. His research interests cover active matter, self assembly, smart and biomimetic materials, and biomedical applications of synthetic microswimmers.

$$F = -\left\langle V(t) \nabla \mathrm{p}(\mathrm{r},\mathrm{t}) \right\rangle = -\left(\frac{\pi p_0^2 V \beta_w}{2\lambda} \right) \Phi(\beta, \rho) \sin(2kd) \tag{2}$$

where k is the wave number, λ is the wavelength, V is the volume of the particle, and d is the distance between the particle and the node or antinode, respectively. The magnitude of the force is proportional to the square of the pressure amplitude p_0 and the volume of the particle V, which is proportional to the third power of the size of the microparicles. This scaling means that smaller particles (especially those less than 1 μm) are harder to manipulate with acoustic radiation forces, but more prone to viscous drag forces, which is proportional to the surface area (scaled to the second power of the size) of the particle.

In Equation (2), the term $\Phi(\beta{\cdot}\rho)$ describes the relationship between the density and compressibility between the particle and the medium, which plays a role in determining the direction of the radiation force. It is given by

$$\Phi(\beta, \rho) = \frac{5\rho_c - 2\rho_w}{2\rho_c + \rho_w} - \frac{\beta_c}{\beta_w} \tag{3}$$

where ρ_c and ρ_w are the density of the particle and medium, respectively, and β_c and β_w are the compressibility of the particle and medium, respectively. If $\Phi(\beta.\rho) > 0$, the particle will be forced to the pressure nodes; otherwise, it will be moved to the pressure antinodes.

In general, particles with higher density and lower compressibility than the medium will move to the pressure nodes in water, such as polystyrene microspheres, metallic microrods, and cells (**Figure 1**), whereas lighter particles with

DOI: 10.1002/smll.201403621

Table 1. A brief comparasion of some common synthetic microswimmer systems.

Propulsion mechanism	Common types	Working principles	Advantages	Limitations
Self-electrophoresis	Bimetallic microrods,[17] Janus microspheres,[75] carbon fibers[25]	Swimmers move by a self-generated electric field created by asymmetric surface electrochemical reactions.	Mechanism well understood; swimmer surface available for functionalization; rich physics.	Very sensitive to solution conductivity; relatively slow swimmer speed (up to ≈100 μm s^{-1}); fuel not biocompatable (H_2O_2, N_2H_4).
Self-diffusiophoresis	Irregularly shaped microparticles (TiO_2, AgCl),[49,76] Janus microspheres (SiO_2 beads half-coated with Pt)[77]	Swimmers move in a self-generated concentration gradient of ions or nonelectrolytes.	Wider selection of "fuels" (UV light, chemicals); Easy to induce long-range particle–particle interactions.	Relatively slow swimmer speed; chemical fuel not biocompatable (often H_2O_2); mechanism still debatable for some swimmers (such as Pt coated SiO_2).[78,79]
Bubble propulsion	Metal microtubes,[31] Janus microspheres,[30] Pt-loaded stomatocytes[80]	Swimmers catalyze the decomposition of chemical fuels, which produces bubbles. The bubble ejection transfers momentum to the swimmer.	High power output and high speed (up to mm s^{-1}); swimmer surface available for functionalization.	Many are large; the production of bubbles is not necessarily desirable; many require toxic fuels such as H_2O_2; bubble ejection often leads to irregular trajectories such as circles and spirals.
Magnetic rotation	Flexible microwires and microchains;[32,37] microhelix[35,36]	The swimmer body rotates in an external magnetic field, which translates into directional motion.	Energy source biocompatible at low power levels; the speed and directionality of the motors are relatively easy to control.	Swimmers are difficult to fabricate and require particular shapes and composition; relatively slow; swimmers move in concert and not autonomously
Electric field	Nanowire diodes in AC field;[44] conducting microparticles in DC fields[46]	A diode can convert AC field into local DC field and move by electroosmosis; Local electrolysis of water on the surface of conducting particles leads to bubble propulsion.	Both systems are fuel-free and can be manipulated externally. AC field is potentially biocompatible.	DC field is not biocompatible, and the voltage required to drive particles is high. Bubbles are not desirable in biological environments. Nanowire diodes are sensitive to ionic strength, and the swimmer speed is low.
Ultrasound	Metallic microparticles[57]	Swimmers locally convert resonating ultrasound into directional motion and spinning.	Swimmers move autonomously; relatively fast (up to a few hundreds μm s^{-1}); rich modes of motion (linear and circular motion, spinning); biocompatable.	Propulsion mechanism not well understood; ultrasound setup not optimized and swimmer behaviors difficult to predict.

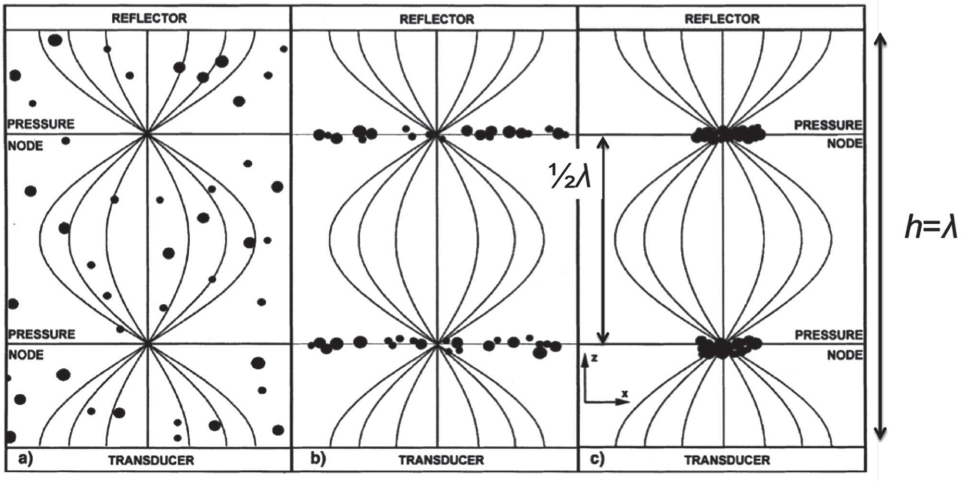

Figure 1. A cartoon illustration of the accumulation of microparticles at the nodal planes by acoustic radiation forces. The acoustic chamber is made of a transducer at the bottom and a reflector at the top. The chamber height h is equal to the sound wavelength λ, thus establishing a standing wave with two nodal planes (Equation (1), $n = 2$). Particles that are initially in a homogeneous distribution within the chamber (a) begin to move and concentrate on the nodal plane when the standing wave is formed (b), and eventually form clumps within the nodal plane (c). Reproduced with permission.[87] Copyright 2003, John Wiley & Sons, Inc.

small 2015,
DOI: 10.1002/smll.201403621

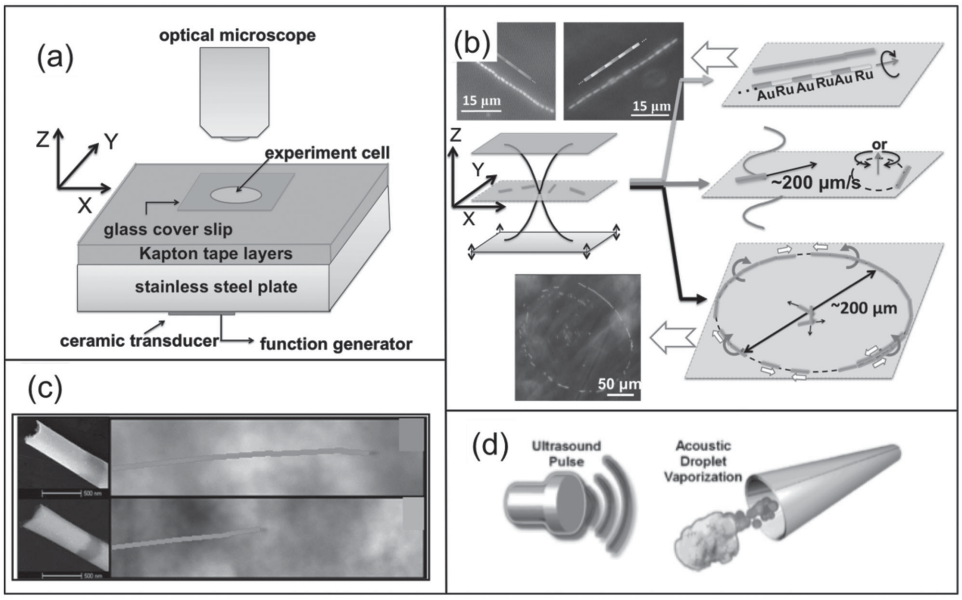

Figure 2. Mechanisms for ultrasound-powered microswimmers. a) Experimental setup of microswimmers propelled by ultrasonic standing waves. Reproduced with permission.[57] Copyright 2012, the American Chemical Society. b) Behavior of microswimmers in an ultrasonic standing wave that includes chaining and spinning (top), fast directional motion (center), and alignment into ring patterns (bottom). Reproduced with permission.[57] Copyright 2012, the American Chemical Society. c) Microswimmers with more concave ends (left column, SEM images) move faster (right column, microscope images with swimmer trajectories), Reproduced with permission.[70] Copyright 2013, the American Chemical Society. d) Microtubes can be propelled by ultrasound via acoustic vaporization of polymers loaded inside the tube. Reproduced with permission.[58] Copyright 2012, John Wiley & Sons, Inc.

a flexible surface are more likely to gather at the pressure antinodes, such as some lipid particles and air bubbles in water.[88] In addition, when multiple particles are exposed to an acoustic wave field in a fluid medium, the particles also experience the secondary radiation force caused by the scatter waves re-radiated by nearby particles. The magnitude of the secondary radiation force increases with the decrease of the interparticle distances.[89]

Microparticles with sizes far smaller than the wavelength of the soundwaves can hardly be manipulated by the acoustic radiation force, as its magnitude decreases sharply as the size of the particle decreases (Equation (2)). However, acoustic streaming, an effect caused by the steady current in a fluid driven by the absorption of high-amplitude acoustic oscillations, can induce hydrodynamic drag forces on microparticles and significantly affect their behavior in the medium. For example, there have been reports on the successful manipulation of silver nanowires and nanoscale bioparticles via the microvortex caused by the vibrating needle[90] and plate,[91] respectively.

3. Acoustic Propulsion

It has long been known and observed that ultrasound, especially in the form of standing waves, can move micro- or nanoparticles. However, it was not until very recently that the autonomous propulsion of individual microparticles by ultrasound was demonstrated. This was first achieved in 2012 by Mallouk, Hoyos, and co-workers[57] where they observed a rich variety of previously unreported behavior in metallic microrods (2 μm long and 330 nm diameter) in ultrasonic standing waves operating in the MHz frequency range. The microrods were synthesized by template-assisted electrodeposition, in which metal ions were electrochemically reduced inside regular and thin nanopores of an anodized alumina oxide (AAO) membrane. The experiment was conducted in a homemade chamber (**Figure 2**a) constructed with a few layers of Kapton tape (whose thickness determined the acoustic chamber height) attached to a stainless steel plate. A piece of PZT ceramic transducer was glued to the back of the steel plate using epoxy resin, and was controlled by a waveform-function generator. Electric signals (typically sine waves) are converted by the piezoelectric effect into mechanical vibrations of the ceramic disk, which translates into an ultrasound wave propogating in water in the acoustic chamber. In this setup, the frequency is often around 3 MHz, which produces a ultrasonic standing wave of one nodal plane located at the center of a chamber 200 μm thick (Equation (1), $\lambda \approx 400$ μm). This experimental setup has been adopted by other research groups in subsequent studies. The observed behaviors of ultrasound-powered microswimmers included levitation, fast and autonomous propulsion ($Re \approx 10^{-5}$), in-plane rotation, fast axial spinning, alignment into ring patterns, and dynamic self-assembly (Figure 2b). Importantly, they noted that both the shape and composition of the particles played significant roles in their propulsion, since only rod-shaped metallic particles demonstrated fast and directional motion whereas polymer rods did not. Another important finding was that the metallic rods driven by ultrasound were capable of maintaining their motion in high salt environments (such as phosphate buffered saline solution), opening up possibilities for them to be used in biologically relevant media.

The mechanism responsible for this dynamic behavior of metallic microrods in ultrasonic waves is clearly of great

DOI: 10.1002/smll.201403621

importance. The origin of the levitation force is well known in acoustics literature, and is generally attributed to the first order or primary acoustic radiation force exerted on the particles (*xy* plane) by sound propagation perpendicular to the substrate (*z* direction). Since the acoustic pressure is at its minimum in the nodal plane (*xy* plane), particles are trapped in that plane, as shown in Figure 2b. According to Equation (1), the nodal plane was designed to have a height of $\lambda/4$, namely, half the height of the acoustic chamber ($n = 1$). The assembly of metallic rods and spheres into well-aligned chains might be caused in part by the attractive second order radiation force induced by the scattered waves from adjacent particles. A number of possible mechanisms also have been proposed to explain specifically the translational motion of these microparticles. The current front-runner of propulsion mechanisms that seems most probable is based on the shape asymmetry of the microparticles. Specifically, a few groups have provided experimental and theoretical support to the idea that the concavity of the microrod tips eventually leads to the directional motion. On the experimental side, this was first proposed by Wang et al.[57] in their original paper. They observed that segmented metal rods (gold–platinum or gold–ruthenium) always moved with one end leading (Pt for AuPt and Ru for AuRu rods). Additionally, when these metallic rods assembled into long chains, they would align into head-to-tail alternating structures (AuRu|AuRu|AuRu…, for example). By carefully examining the morphology of the rods under scanning electron microscope (SEM), it was revealed that these rods, which were fabricated via template-assisted electrodepositon, had one end (usually gold) consistently of concave shape. This is possibly related to the wetting behavior of the plating solutions inside the narrow pores in the template membrane.

The role of shape asymmetry in the ultrasonic propulsion of metallic microrods was further supported by a subsequent study from Wang's group at University of California, San Diego, where Au/Ni/Au nanowires were employed for axial propulsion.[70] By putting polystyrene nanospheres into the cylindrical nanopores of the AAO membrane during electrodeposition, nanorods with more concave ends could be fabricated. The authors noticed that an increase of speed up to 67% from 152.7 to 254.9 μm s^{-1} was achieved by microrods with higher concavity (i.e., the ones fabricated by templates infiltrated with nanospheres) at a transducer voltage of 10 V (Figure 2c). Although neither of these two works could theoretically explain how end concavity leads to the directional propulsion of metallic microrods, they intuitively described a process where concave and convex ends would scatter incident ultrasound waves differently, thus creating an acoustic pressure difference between the two ends of the rods, which leads to unidirectional motion.

The propulsion mechanism of metallic microrods in standing ultrasonic waves was recently examined more closely from a theoretical perspective by Nadal and Lauga.[71] They proposed a new theory based on asymmetric local streaming, and provided a rigid theoretical framework to describe the process by which the small amplitude oscillation of rigid bodies in a standing wave can translate, via shape asymmetry-induced local acoustic streaming effects, into motion in a direction perpendicular to the acoustic wave. Based on their calculation, a roughly spherical particle with an aspect ratio of 10 in a standing acoustic wave could be propelled at ≈26 μm s^{-1} in conditions similar to those used by a previous group.[57] Although this value is one order of magnitude smaller than the experimentally measured particle speed (up to 200 μm s^{-1}), the theoretical framework established by Nadal and Lauga[71] has laid the foundation for a more coherent and accurate theory.

Despite the improved understanding gained from experimental and theoretical investigations into the mechanism responsible for the axial propulsion of ultrasound-powered microswimmers, the origins of other modes of motion are still elusive. For example, it is commonly observed that, besides the axial directional motion, microswimmers in an acoustic chamber undergo fast spinning around the long axis, and this is particularly noticeable for those that are aligned in chains (Figure 2b, top). Near the spinning chains, microswimmers and tracer particles alike are dragged by the strong vortex and rotate around the chain. This was the focus of a recent study by Stavis and co-workers,[92] in which high-speed cameras were combined with particle-tracking analysis to determine that the microswimmers could spin as fast as 1000 revolutions per second. In addition, their analysis revealed that the spinning and translational motions of the same microswimmer were decoupled, indicating that two different mechanisms were possibly responsible for each of these modes of motion. Besides the axial spinning, microswimmers in an ultrasound field also demonstrate fast in-plane rotation and, like the spinning effect, this phenomenon is not understood.

At the end of this section on acoustic propulsion, we would like to briefly mention an entirely different ultrasonically propelled microswimmer system reported by Kagan et al. in 2012.[58] Here, the authors demonstrated that metallic microtubes of micrometers in length travelled with impressive speeds of up to 6.3 m s^{-1} with a high pressure (3.8 MPa) at a short ultrasound pulse (4.4 ms) (Figure 2d). These microbullets take advantage of the vaporization of perfluorocarbons (PFCs) that are loaded inside the conically shaped microtubes, and can be potentially used for directed drug delivery or penetration into tissues. Although ultrasound is used in this propulsion system, its only function is to vaporize droplets embedded inside microtubes. Therefore, the propulsion is ultimately provided by the ejection of gas bubbles of vaporized PFCs, and this swimmer is essentially the same as other bubble-propelled microswimmers.

4. Functionalization and Applications of Ultrasonically Propelled Microswimmers

For machines to be useful at the nano- and microscales where Brownian motion has a significant impact on the direction and speed of moving objects, some form of external or autonomous directional guidance is often needed. This is commonly achieved by incorporating the microswimmers with magnetic materials such as Fe_3O_4 and nickel. The swimmer is therefore steered by aligning the magnetic components in an external magnetic field (usually Neodymium magnets) (**Figure 3**a). A few studies have demonstrated external steering of microswimmers propelled in ultrasound by

DOI: 10.1002/smll.201403621

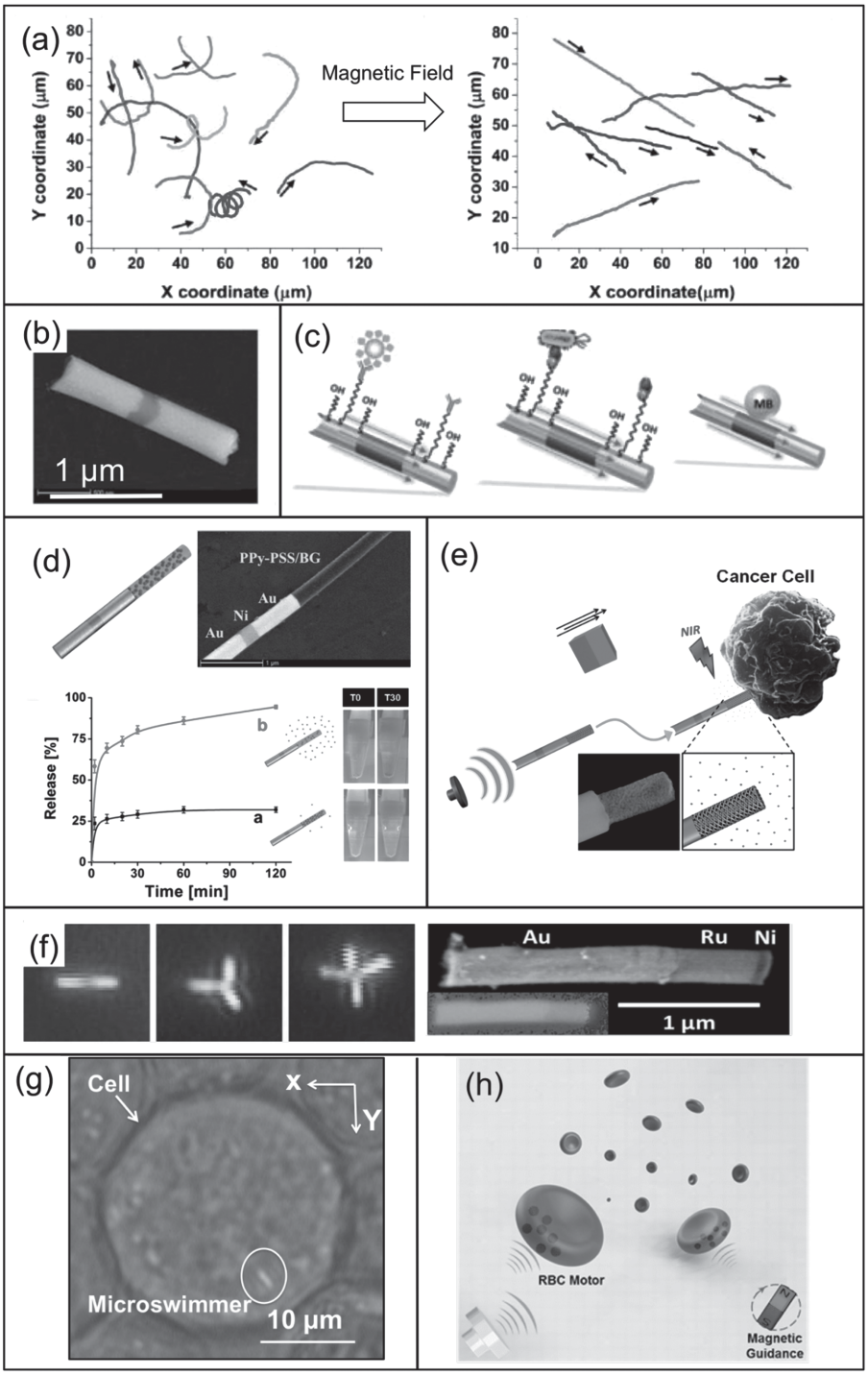

Figure 3. Functionalization and applications of ultrasound-powered microswimmers. a) When an external magnetic field is applied, the trajectories of microswimmers embedded with magnetic materials change from random (left) to straight lines (right). Reproduced with permission.[69] Copyright 2012, the American Chemical Society. b) SEM of a gold (bright) nanowire with a nickel segment (dark) in the middle. The Ni segment renders the microrod susceptible to external magnetic fields. c) Ultrasound-powered microswimmers can capture and transport *E. coli* (left), *S. aureus* (center), and magnetic microspheres (right) via correct surface functionalizations or magnetic interactions. d) The PPy–PSS segment in an ultrasound powered microswimmer can release bright green molecules in an acidic environment. The plot shows the release at pH = 4 (b) and pH = 7.4 (a). Panels (b,c,d) reproduced with permission.[70] Copyright 2012, the American Chemical Society. e) The porous gold segment in an ultrasound-powered microswimmer can release doxorubicin near a HeLa cell when irradiated by NIR light. Reproduced with permission.[67] Copyright 2014, John Wiley & Sons Inc. f) Ultrasound-powered microswimmers can dynamically assemble into dimers, trimers, and multimers via magnetic interactions. Left: Optical micrographs showing the assembly process; right: an SEM image and element mapping of a Au/Ru/Ni microrod in the optical image. Reproduced with permission.[94] Copyright 2014, the American Chemical Society. g) Microswimmers can be activated inside a living HeLa cell by ultrasound waves. Reproduced with permission.[68] Copyright 2014, John Wiley & Sons Inc. h) Microswimmers made of red blood cells internalized with magnetic nanoparticles. Reproduced with permission.[95] Copyright 2014, American Chemical Society.

DOI: 10.1002/smll.201403621

incorporating a Ni segment in the metallic nanorods during the electrodeposition process. For example, Garcia-Gradilla et al.[70] fabricated gold nanowires with a Ni segment sandwiched in between (Figure 3b). The Ni segment also allowed the capture and transfer of magnetic particles by microswimmers via simple magnetic interactions (Figure 3c, right panel). A similar experiment by Ahmed et al.[69] showed that Ru/Ni/Au nanowire swimmers with a short Ni segment (40 ± 5 nm) in the middle could be externally steered to target live HeLa cells in vitro with micrometer-level precision at speeds up to 180 μm s^{-1}. In both studies, the magnetic field was not found to significantly affect the swimmer's ability to move, while easy and precise control over their directions could generally be achieved. We would like to briefly note that it is desirable to design microswimmers that do not require external fields to steer, but rather that are capable of mapping the route and finding targets on their own. In this regard, chemotaxis of synthetic microswimmers along particular chemical gradients could prove very useful, especially in tumor microenvironments where the local pH is significantly more acidic than in normal parts of the human body.[93]

Designing microswimmers that are capable of loading and transporting microscale targets is of great interest for a wide variety of applications, ranging from biological separation to drug delivery. Previously a number of studies have achieved such capabilities with chemically propelled microswimmers that move in self-generated gradients,[96–98] or are propelled by ejecting bubbles.[99–101] However, these microswimmers require toxic chemicals such as hydrogen peroxide (H_2O_2), and are therefore not biocompatible. Ultrasound-powered microswimmers are fuel-free and can move at a relatively high speed and, with proper engineering, can be used as an ideal microscale carrier. A set of preliminary experiments on this front was carried out by functionalizing Au/Ni/Au microswimmer surfaces with self-assembled monolayers (SAM) of organic chains with thiol ends,[70] taking advantage of the strong gold–sulfur chemistry which has proved effective in previous microswimmer transport studies.[102] The lectin and antiprotein A antibody bioreceptors on the SAM layer allowed for the capture and transport of *E. coli* and *S. aureus* bacteria effectively via strong and specific receptor–bacteria interactions (Figure 3c, left and center panels). Importantly, it was found that the speeds of ultrasound-powered microswimmers did not see significant changes after the surface functionalization, in clear contrast to the reduced speeds of chemically propelled microswimmers modified with SAMs. Such insensitivity towards surface modification, as well as their capability to move in various biological fluids, equips ultrasound-powered microswimmers with unique advantages for biomedical applications.

In addition to loading and transporting microparticles, ultrasonically driven microswimmers are also an attractive option for delivering therapeutic drugs. The first example was demonstrated by Garcia-Gradilla et al.,[70] who showed that metallic microswimmers with a polypyrrole–polystyrene sulfonate (PPy–PSS) segment could be used as a carrier to deliver antiseptic drugs (Figure 3d). In this experiment the polymer segment became protonated when the microswimmer was exposed to an acidic environment (pH < 4), thus releasing the brilliant green (BG) drug that was electrostatically attached to the polymer surface. Within 120 min, up to 95% of the drugs was released. Remarkably, the electrodeposited PPy–PSS segment remained intact and well connected to the rest of the microswimmer after 30 min of ultrasound operation. In a more recent study, a porous gold segment instead of a polymer segment was used to encapsulate and release drugs on environmental cues by ultrasound-powered Au/Ni/Au microswimmers (Figure 3e).[67] The porous gold segment was fabricated by dealloying electrodeposited gold–silver alloy in nitric acid, and was further coated with polyelectrolytes. Anticancer drug molecules (doxorubicin, DOX) then electrostatically attached to the anionic polymeric pores on the microswimmers. One particular benefit of the porous structure was a 20-fold increase in surface area that was available for the drugs to attach to, thus dramatically increasing the amount of drugs for delivery (up to 13.4 μg mg^{-1}). With the help of an external magnetic field, the microswimmer was steered at speeds of around 60 μm s^{-1} to the vicinity of a HeLa cell suspended in a phosphate buffered saline solution. Upon excitation with NIR irradiation at 808 nm, the porous gold nanostructure exhibited a strong photothermal effect, leading to heat-induced structural changes of the polymeric coatings. As a result, up to 40% of DOX drug molecules could be released within 120 min. Although the successful demonstration of controlled transport and release of anticancer drugs near a cancer cell is promising, one piece missing from the puzzle is how effective the operation was in killing the cancer cell, which was not discussed in the above study.

Besides operating as drug carriers and delivering the drug near cancer cells, ultrasound-powered microswimmers can also be implanted inside living cancer cells, taking advantage of the cell's ability to engulf foreign objects via phagocytosis. This was demonstrated in a recent study from Mallouk and co-workers,[69] in which they discovered that gold nanorods were internalized by HeLa cancer cells after 24 h of incubation (Figure 3g). Once inside the cell, these microswimmers could be activated by ultrasonic standing waves. Due to the possible damping from the cell membrane and the elevated viscosity of the cytoplasm, these internalized microswimmers moved significantly slower than when they were outside the cells (≈60 μm s^{-1} vs ≈100 μm s^{-1}). What was interesting was that the microswimmers moved in two modes inside cells, namely, axial propulsion and spinning, and in both modes clear interactions were observed between the microswimmers and cell components (cell membrane or subcellular organelles). This suggests possible uses for these ultrasound-powered microswimmers as intracellular probes or tools to investigate and agitate cells from within, something that has proved difficult but useful for cell biologists and bioengineers alike. In addition to the propulsion inside living cells, the authors also studied the strong binding effects between ultrasound-powered microswimmers and the exterior of cancer cells, and compared it to the minimal binding observed between microswimmers and red blood cells as well as polystyrene microspheres. This information has important implications for biomedical applications involving the movement of microswimmers inside blood streams.

small 2015,
DOI: 10.1002/smll.201403621

Building upon the success of driving microswimmers inside living cancer cells, a recent study by Wang and coworkers demonstrated microswimmers made of natural red blood cells (Figure 3h).[95] In their experiment, iron oxide nanoparticles were loaded into red blood cells by the hypotonic hemolysis process, and the resulting modified red blood cells could be propelled by ultrasound and steered by an external magnetic field. Although the capability of magnetic steering with magnetic nanoparticles was obvious and well established, the acoustic propulsion of red blood cells was quite surprising and was attributed to an uneven distribution of nanoparticles inside the cells. Such a proposed propulsion mechanism, however, seems to contradict previous experiments where hard materials and shape asymmetry are required for acoustic microswimmers. Therefore a more thorough study on the propulsion mechanism of red blood cell microswimmers in ultrasound is needed. Despite a relatively slow speed (≈10 μm s^{-1}) and the unclear propulsion mechanism, these microswimmers made of red blood cells represent an important step forward in achieving the ultimate biocompatible microswimmers, taking advantage of what is available in nature.

Not only can ultrasound provide propulsion to microswimmers, it can also be used as an active component in driving the self assembly of microparticles. For example, a recent study by Ahmed et al. showed that metallic rod-shaped microswimmers with a ferromagnetic nickel segment could in an ultrasound field dynamically self-assemble into dimers, trimers and multimers (Figure 3f).[94] In this experiment, the attraction among individual units (nanorods) originated from the magnetic interactions between the Ni segments in each nanorod, while the relative speeds of each microswimmer served as the repulsive interactions that pulled the units apart. Therefore, by tuning the magnitude of the ultrasound applied, which affects the speeds of microswimmers, the degree of assembly could be controlled and assemblies of different numbers of units could be obtained. This work demonstrates the power of combining ultrasound propulsion with magnetic interactions between individual microswimmers, while two recent further works showed that microrods driven by both ultrasound and chemical fuels exhibit reversible and dynamic assembly. Wang et al.[103] and Xu et al.[104] independenty reported that microrods exposed to ultrasound and H_2O_2 solution can switch between a swarming state and a free state by turning the ultrasound on or off, respectively. In addition, Wang et al. achieved the forward–backward shuttling of AuRu microrods, while Xu et al. demonstrated that a swarm of AuPt microswimmers can be collectively transported by varying the ultrasound frequency. These two works represent the latest advances in manipulating a group of microswimmers by ultrasound.

5. Conclusions and Outlook

The discovery of ultrasonic propulsion has marked a new phase in the research of self-propelled synthetic microswimmers. Ultrasonic propulsion, being inherently safe, biocompatible, and versatile, offers tremendous benefits if used as the propulsion mechanism of micromachines in biomedical scenarios and, thus, has attracted wide attention in research communities spanning acoustics, bioengineering, colloidal physics, nanotechnology, and cell biology, among others. Thanks to the ever-increasing efforts since the discovery of the first ultrasonically propelled microswimmers in 2012, we now have a better understanding of how ultrasound propels colloidal particles into directional motion. In addition, a number of promising, although primitive, functionalities have been successfully demonstrated, including external steering by magnetic fields, capture and transport of specific cargos, controlled drug release, and activation inside live cells. All these achievements bring us closer to realizing the *Fantastic Voyage* dream, where artificial micromachines are used to carry out medical operations inside human bodies.

However, in order to bring the visions of Richard Feynman and *Fantastic Voyage* into reality, a number of critical challenges facing ultrasonically propelled microswimmers must be addressed. These include:

1. The elucidation of the propulsion mechanism of microswimmers in ultrasonic standing waves, which is crucial for the development of such systems into a mature and useful platform. The recent theoretical framework proposed by Nadal and Lauga[71] represents a solid step forward in this direction; however, this work does not cover the fast spinning of metallic microrods, which is another prominent behavior of these rods. In addition, it is interesting to see how their theory can be verified or challenged by further experiments that will need to emphasize finer control over the parameters of the microparticles, soundwaves, and the general experimental setup. Numerical simulations could also prove useful in addressing this challenge.
2. The precise control of speed and direction, as well as modes of motion, of ultrasonically propelled microswimmers. In order for these microswimmers to carry out biological functions, it is crucial to be able to control their motion as precisely as possible to maximize efficacy. The current experimental technique yields ultrasonic microswimmers traveling at maximum speeds of ≈250 μm s^{-1}, which can be modulated by varying the applied voltage on the transducer. However, an even higher swimmer speed is greatly desired not only to reduce the operational ultrasound power (therefore minimizing damage to tissues and cells), but also to equip the swimmer with the ability to overcome blood flows when needed. The direction of these swimmers, on the other hand, can be externally controlled by magnetic fields. But it is highly desirable to design microswimmers that can sense and move towards targets autonomously instead of being externally steered, especially in complicated environments such as human bodies where constant and precise external steering becomes challenging. Lastly, the fast axial spinning of metallic microrods in ultrasound can be a powerful tool for biological applications if used properly, yet thus far little has been exploited from this mode of motion. This is most likely due to a mixture of technical difficulty and lack of theoretical understanding of this spinning phenomenon.
3. In vitro and in vivo experiments demonstrating the feasibility of ultrasonic microswimmers for biomedical

applications. The true test of the claim that ultrasonically propelled microswimmers are useful for biomedical applications lies in successfully achieving planned functionalities in real-world scenarios. The first step of demonstrating this capability would be in vitro experiments in biologically relevant environments. Although much progress has been made in this aspect that includes experiments with ultrasonic microswimmers in various liquid media (phosphate buffered saline, serum, and saliva)[70] and experiments demonstrating the interaction of microswimmers with live cells,[67–69] there is still a noticeable lack of discussion of if and how microswimmers can be propelled by ultrasound to move in environments like blood vessels where complicated branching, high viscosity, dense blood cell populations, and high fluid speeds can pose significant challenges to microswimmers.

Although faced with these challenges, ultrasonically propelled microswimmers hold significant promise in inspiring the design of intelligent, multifunctional, and biomimetic micromachines that can find wide uses in sensing, analytical chemistry, drug delivery, environmental monitoring and remediation, minimally invasive surgery, and much more.

Acknowledgements

W. Wang is supported by National Natural Science Foundation of China (Grant No. 11402069) and Shenzhen Peacock Technological Innovation Program (Grant No. KQCX20140521144102503). F. Li, L. Meng, H. Zheng, and F. Cai were supported by National Natural Science Foundation of China (Grant Nos. 11274008, 11325420, 11304341,11404363) and 973 Program (Grant No. 2015CB755500). F. Li was partially supported by China Postdoctoral Science Foundation 2014M560682.

[1] G. M. Whitesides, *Sci. Am.* **2001**, *285*, 78.
[2] G. A. Ozin, I. Manners, S. Fournier-Bidoz, A. Arsenault, *Adv. Mater.* **2005**, *17*, 3011.
[3] R. P. Feynman, *Engineering Sci.* **1960**, *23*, 22.
[4] IMDB Fantastic Voyage. http://www.imdb.com/title/tt0060397/, accessed: March, 2015.
[5] R. E. Smalley, *Sci. Am.* **2001**, *285*, 76.
[6] T. E. Mallouk, A. Sen, *Sci. Am.* **2009**, *5*, 72.
[7] S. Sengupta, M. E. Ibele, A. Sen, *Angew. Chem. Int. Ed.* **2012**, *51*, 8434.
[8] M. Guix, C. C. Mayorga-Martinez, A. Merkoci, *Chem. Rev.* **2014**, *114*, 6285.
[9] R. Kapral, *J. Chem. Phys.* **2013**, *138*, 020901.
[10] D. Patra, S. Sengupta, W. T. Duan, H. Zhang, R. Pavlick, A. Sen, *Nanoscale* **2013**, *5*, 1273.
[11] W. Gao, J. Wang, *Nanoscale* **2014**, *6*, 10486.
[12] E. M. Purcell, *Am. J. Phys.* **1977**, *45*, 3.
[13] M. Tanase, E. J. Felton, D. S. Gray, A. Hultgren, C. S. Chen, D. H. Reich, *Lab Chip* **2005**, *5*, 598.
[14] P. A. Smith, C. D. Nordquist, T. N. Jackson, T. S. Mayer, B. R. Martin, J. Mbindyo, T. E. Mallouk, *Appl. Phys. Lett.* **2000**, *77*, 1399.
[15] C. Gosse, V. Croquette, *Biophys. J* **2002**, *82*, 3314.
[16] D. Fan, F. Zhu, R. Cammarata, C. Chien, *Appl. Phys. Lett.* **2004**, *85*, 4175.
[17] W. F. Paxton, K. C. Kistler, C. C. Olmeda, A. Sen, S. K. St Angelo, Y. Cao, T. E. Mallouk, P. E. Lammert, V. H. Crespi, *J. Am. Chem. Soc.* **2004**, *126*, 13424.
[18] S. Fournier-Bidoz, A. C. Arsenault, I. Manners, G. A. Ozin, *Chem. Commun.* **2005**, 441.
[19] W. Wang, W. Duan, S. Ahmed, T. E. Mallouk, A. Sen, *Nano Today* **2013**, *8*, 531.
[20] P. H. Colberg, S. Y. Reigh, B. Robertson, R. Kapral, *Acc. Chem. Res.* **2014**, 12, , 3504.
[21] S. Sengupta, D. Patra, I. Ortiz-Rivera, A. Agrawal, S. Shklyaev, K. K. Dey, U. Cordova-Figueroa, T. E. Mallouk, A. Sen, *Nat. Chem.* **2014**, *6*, 415.
[22] W. Duan, R. Liu, A. Sen, *J. Am. Chem. Soc.* **2013**, *135*, 1280.
[23] R. Liu, A. Sen, *J. Am. Chem. Soc.* **2011**, *133*, 20064.
[24] D. Pantarotto, W. R. Browne, B. L. Feringa, *Chem. Commun.* **2008**, 1533.
[25] N. Mano, A. Heller, *J. Am. Chem. Soc.* **2005**, *127*, 11574.
[26] T. R. Kline, W. F. Paxton, T. E. Mallouk, A. Sen, *Angew. Chem. Int. Ed.* **2005**, *117*, 754.
[27] W. F. Paxton, P. T. Baker, T. R. Kline, Y. Wang, T. E. Mallouk, A. Sen, *J. Am. Chem. Soc.* **2006**, *128*, 14881.
[28] J. Wu, S. Balasubramanian, D. Kagan, K. M. Manesh, S. Campuzano, J. Wang, *Nat. Commun.* **2010**, *1*, 36.
[29] C. Stock, N. Heureux, W. R. Browne, B. L. Feringa, *Chem. Eur. J.* **2008**, *14*, 3146.
[30] J. G. Gibbs, Y. P. Zhao, *Appl. Phys. Lett.* **2009**, *94*, 163104.
[31] A. A. Solovev, Y. Mei, E. Bermúdez Ureña, G. Huang, O. G. Schmidt, *Small* **2009**, *5*, 1688.
[32] W. Gao, S. Sattayasamitsathit, J. Orozco, J. Wang, *J. Am. Chem. Soc.* **2011**, *24*, 11862.
[33] R. Dreyfus, J. Baudry, M. L. Roper, M. Fermigier, H. A. Stone, J. Bibette, *Nature* **2005**, *437*, 862.
[34] L. Zhang, J. J. Abbott, L. Dong, K. E. Peyer, B. E. Kratochvil, H. Zhang, C. Bergeles, B. J. Nelson, *Nano. Lett.* **2009**, *9*, 3663.
[35] A. Ghosh, P. Fischer, *Nano. Lett.* **2009**, *9*, 2243.
[36] S. Tottori, L. Zhang, F. Qiu, K. K. Krawczyk, A. Franco-Obregon, B. J. Nelson, *Adv. Mater.* **2012**, *24*, 811.
[37] W. Gao, S. Sattayasamitsathit, K. M. Manesh, D. Weihs, J. Wang, *J. Am. Chem. Soc.* **2010**, *132*, 14403.
[38] L. Zhang, T. Petit, Y. Lu, B. E. Kratochvil, K. E. Peyer, R. Pei, J. Lou, B. J. Nelson, *ACS Nano* **2010**, *4*, 6228.
[39] D. Fan, F. Zhu, R. Cammarata, C. Chien, *Phys. Rev. Lett.* **2005**, *94*, 247208.
[40] B. Edwards, N. Engheta, S. Evoy, *J. Appl. Phys.* **2007**, *102*, 024913.
[41] S. T. Chang, V. N. Paunov, D. N. Petsev, O. D. Velev, *Nat. Mater.* **2007**, *6*, 235.
[42] D. Fan, R. Cammarata, C. Chien, *Appl. Phys. Lett.* **2008**, *92*, 093115.
[43] D. Fan, Z. Yin, R. Cheong, F. Q. Zhu, R. C. Cammarata, C. Chien, A. Levchenko, *Nat. Nanotechnol.* **2010**, *5*, 545.
[44] P. Calvo-Marzal, S. Sattayasamitsathit, S. Balasubramanian, J. R. Windmiller, C. Dao, J. Wang, *Chem. Commun.* **2010**, *46*, 1623.
[45] G. Loget, A. Kuhn, *J. Am. Chem. Soc.* **2010**, *132*, 15918.
[46] G. Loget, A. Kuhn, *Nat. Commun.* **2011**, *2*, 535.
[47] K. Kim, X. Xu, J. Guo, D. Fan, *Nat.Commun.* **2014**, *5*.
[48] X. Xu, K. Kim, D. Fan, *Angew. Chem. Int. Ed.* **2015**, *54*, 2525.
[49] Y. Hong, M. Diaz, U. M. Córdova-Figueroa, A. Sen, *Adv. Funct. Mater.* **2010**, *20*, 1568.
[50] M. Liu, T. Zentgraf, Y. Liu, G. Bartal, X. Zhang, *Nat. Nanotechnol.* **2010**, *5*, 570.
[51] M. Ibele, T. E. Mallouk, A. Sen, *Angew. Chem. Int. Ed.* **2009**, *48*, 3308.

DOI: 10.1002/smll.201403621

[52] J. P. Abid, M. Frigoli, R. Pansu, J. Szeftel, J. Zyss, C. Larpent, S. Brasselet, *Langmuir* **2011**, *27*, 7967.
[53] J. Cheng, S. Sreelatha, R. Hou, A. Efremov, R. Liu, J. R. van der Maarel, Z. Wang, *Phys. Rev. Lett.* **2012**, *109*, 238104.
[54] M. Liu, R. Hou, J. Cheng, I. Y. Loh, S. Sreelatha, J. N. Tey, J. Wei, Z. Wang, *ACS Nano* **2014**, *8*, 1792.
[55] I. Y. Loh, J. Cheng, S. R. Tee, A. Efremov, Z. Wang, *ACS Nano* **2014**, *8*, 10293.
[56] M. You, Y. Chen, X. Zhang, H. Liu, R. Wang, K. Wang, K. R. Williams, W. Tan, *Angew. Chem. Int. Ed.* **2012**, *124*, 2507.
[57] W. Wang, L. A. Castro, M. Hoyos, T. E. Mallouk, *ACS Nano* **2012**, *6*, 6122.
[58] D. Kagan, M. J. Benchimol, J. C. Claussen, E. Chuluun-Erdene, S. Esener, J. Wang, *Angew. Chem. Int. Ed.* **2012**, *51*, 7519.
[59] H. R. Jiang, N. Yoshinaga, M. Sano, *Phys. Rev. Lett.* **2010**, *105*, 268302.
[60] L. Baraban, R. Streubel, D. Makarov, L. Han, D. Karnaushenko, O. G. Schmidt, G. Cuniberti, *ACS Nano* **2012**, *7*, 1360.
[61] B. Qian, D. Montiel, A. Bregulla, F. Cichos, H. Yang, *Chem. Sci.* **2013**, *4*, 1420.
[62] T. Mirkovic, N. S. Zacharia, G. D. Scholes, G. A. Ozin, *ACS Nano* **2010**, *4*, 1782.
[63] L. K. E. A. Abdelmohsen, F. Peng, Y. Tu, D. A. Wilson, *J. Mater. Chem. B* **2014**, *2*, 2395.
[64] J. Wang, W. Gao, *ACS Nano* **2012**, *6*, 5745.
[65] R. S. M. Rikken, R. J. M. Nolte, J. C. Maan, J. C. M. van Hest, D. A. Wilson, P. C. M. Christianen, *Soft Matt.* **2014**, *10*, 1295.
[66] K. E. Peyer, S. Tottori, F. M. Qiu, L. Zhang, B. J. Nelson, *Chem.—Euro. J.* **2013**, *19*, 28.
[67] V. Garcia-Gradilla, S. Sattayasamitsathit, F. Soto, F. Kuralay, C. Yardımcı, D. Wiitala, M. Galarnyk, J. Wang, *Small* **2014**, *10*, 4154.
[68] W. Wang, S. Li, L. Mair, S. Ahmed, T. J. Huang, T. E. Mallouk, *Angew. Chem. Int. Ed.* **2014**, *53*, 3201.
[69] S. Ahmed, W. Wang, L. O. Mair, R. D. Fraleigh, S. Li, L. A. Castro, M. Hoyos, T. J. Huang, T. E. Mallouk, *Langmuir* **2013**, *29*, 16113.
[70] V. Garcia-Gradilla, J. Orozco, S. Sattayasamitsathit, F. Soto, F. Kuralay, A. Pourazary, A. Katzenberg, W. Gao, Y. Shen, J. Wang, *ACS Nano* **2013**, *7*, 9232.
[71] F. Nadal, E. Lauga, *Phys. Fluids* **2014**, *28*, 082001.
[72] H. G. Craighead, *Science* **2000**, *290*, 1532.
[73] E. R. Kay, D. A. Leigh, F. Zerbetto, *Angew. Chem. Int. Ed.* **2007**, *46*, 72.
[74] K. Kinbara, T. Aida, *Chem. Rev.* **2005**, *105*, 1377.
[75] P. M. Wheat, N. A. Marine, J. L. Moran, J. D. Posner, *Langmuir* **2010**, *26*, 13052.
[76] M. Ibele, T. E. Mallouk, A. Sen, *Angew. Chem. Int. Ed.* **2009**, *48*, 3308.
[77] J. Howse, R. Jones, A. Ryan, T. Gough, R. Vafabakhsh, R. Golestanian, *Phys. Rev. Lett.* **2007**, *99*, 048102.
[78] S. J. Wang, N. Wu, *Langmuir* **2014**, *30*, 3477.
[79] S. Ebbens, D. A. Gregory, G. Dunderdale, J. R. Howse, Y. Ibrahim, T. B. Liverpool, R. Golestanian, *EPL* **2014**, *106*, 58006.
[80] D. A. Wilson, R. J. M. Nolte, J. C. M. van Hest, *Nat. Commun.* **2012**, *4*, 268.
[81] J. Friend, L. Y. Yeo, *Rev. Mod. Phys.* **2011**, *83*, 647.
[82] F. E. Borgnis, *Rev. Mod. Phys.* **1953**, *25*, 653.
[83] A. A. Doinikov, *Acoustic Radiation Forces: Classical Theory and Recent Advances: Recent Research Developments in Acoustics*, Transword Research Network, Trivandrum, Kerala, **2003**, p. 39.
[84] L. Meng, F. Y. Cai, Z. D. Zhang, L. L. Niu, Q. F. Jin, F. Yan, J. R. Wu, Z. H. Wang, H. R. Zheng, *Biomicrofluidics* **2011**, *5*, 044104.
[85] X. Y. Ding, S. C. S. Lin, B. Kiraly, H. J. Yue, S. X. Li, I. K. Chiang, J. J. Shi, S. J. Benkovic, T. J. Huang, *Proc. Natl. Acad. Sci. USA* **2012**, *109*, 11105.
[86] H. Bruus, *Lab Chip* **2012**, *12*, 1014.
[87] J. F. Spengler, W. T. Coakley, K. T. Christensen, *AIChE J.* **2003**, *49*, 2773.
[88] T. G. Leighton, A. J. Walton, M. J. W. Pickworth, *Euro. J. Phys.* **1990**, *11*, 47.
[89] A. A. Doinikov, *J. Fluid Mech.* **2001**, *444*, 1.
[90] N. Li, J. H. Hu, H. Q. Li, S. Bhuyan, Y. J. Zhou, *Appl. Phys. Lett.* **2012**, *101*, 093113.
[91] C. M. Lin, Y. S. Lai, H. P. Liu, C. Y. Chen, A. M. Wo, *Anal. Chem.* **2008**, *80*, 8937.
[92] A. L. Balk, L. O. Mair, P. P. Mathai, P. N. Patrone, W. Wang, S. Ahmed, T. E. Mallouk, J. A. Liddle, S. M. Stavis, *ACS Nano* **2014**, *8*, 8300.
[93] R. K. Jain, T. Stylianopoulos, *Nat. Rev. Clin. Oncol.* **2010**, *7*, 653.
[94] S. Ahmed, D. T. Gentekos, C. A. Fink, T. E. Mallouk, *ACS Nano* **2014**, *8*, 11053.
[95] Z. Wu, T. Li, J. Li, W. Gao, T. Xu, C. Christianson, W. Gao, M. Galarnyk, Q. He, L. Zhang, *ACS Nano* **2014**, *8*, 12041.
[96] D. Kagan, R. Laocharoensuk, M. Zimmerman, C. Clawson, S. Balasubramanian, D. Kang, D. Bishop, S. Sattayasamitsathit, L. Zhang, J. Wang, *Small* **2010**, *6*, 2741.
[97] S. Sundararajan, P. E. Lammert, A. W. Zudans, V. H. Crespi, A. Sen, *Nano Lett.* **2008**, *8*, 1271.
[98] W. Wang, W. Duan, A. Sen, T. E. Mallouk, *Proc. Natl. Acad. Sci. USA* **2013**, *110*, 17744.
[99] M. Guix, J. Orozco, M. Garcia, W. Gao, S. Sattayasamitsathit, A. Merkoci, A. Escarpa, J. Wang, *ACS Nano* **2012**, *6*, 4445.
[100] L. Baraban, D. Makarov, R. Streubel, I. Monch, D. Grimm, S. Sanchez, O. G. Schmidt, *ACS Nano* **2012**, *6*, 3383.
[101] S. Sanchez, A. A. Solovev, S. Schulze, O. G. Schmidt, *Chem. Commun.* **2011**, *47*, 698.
[102] J. Wang, *Lab Chip* **2012**, *12*, 1944.
[103] W. Wang, W. Duan, Z. Zhang, M. Sun, A. Sen, T. Mallouk, *Chem. Commun.* **2015**, *51*, 1020.
[104] T. Xu, F. Soto, W. Gao, R. Dong, V. Garcia-Gradilla, E. Magaña, X. Zhang, J. Wang, *J. Am. Chem. Soc.* **2015**, *137*, 2163.

Received: December 5, 2014
Revised: February 25, 2015
Published online: